Elastic Modulus Determination of Normal and Glaucomatous Human Trabecular Meshwork

Julie A. Last,[1] *Tingrui Pan,*[2] *Yuzhe Ding,*[2] *Christopher M. Reilly,*[3] *Kate Keller,*[4] *Ted S. Acott,*[4] *Michael P. Fautsch,*[5] *Christopher J. Murphy,*[*,6,7] *and Paul Russell*[*,7]

Purpose. Elevated intraocular pressure (IOP) is a risk factor for glaucoma. The principal outflow pathway for aqueous humor in the human eye is through the trabecular meshwork (HTM) and Schlemm's canal (SC). The junction between the HTM and SC is thought to have a significant role in the regulation of IOP. A possible mechanism for the increased resistance to flow in glaucomatous eyes is an increase in stiffness (increased elastic modulus) of the HTM. In this study, the stiffness of the HTM in normal and glaucomatous tissue was compared, and a mathematical model was developed to predict the impact of changes in stiffness of the juxtacanalicular layer of HTM on flow dynamics through this region.

Methods. Atomic force microscopy (AFM) was used to measure the elastic modulus of normal and glaucomatous HTM. According to these results, a model was developed that simulated the juxtacanalicular layer of the HTM as a flexible membrane with embedded pores.

Results. The mean elastic modulus increased substantially in the glaucomatous HTM (mean = 80.8 kPa) compared with that in the normal HTM (mean = 4.0 kPa). Regional variation was identified across the glaucomatous HTM, possibly corresponding to the disease state. Mathematical modeling suggested an increased flow resistance with increasing HTM modulus.

Conclusions. The data indicate that the stiffness of glaucomatous HTM is significantly increased compared with that of normal HTM. Modeling exercises support substantial impairment in outflow facility with increased HTM stiffness. Alterations in the biophysical attributes of the HTM may participate directly in the onset and progression of glaucoma. (*Invest Ophthalmol Vis Sci.* 2011;52:2147–2152) DOI:10.1167/iovs.10-6342

Glaucoma is the leading cause of irreversible blindness, affecting nearly 70 million people worldwide. The only known treatable risk factor for glaucoma is the elevated intraocular pressure (IOP) caused by an increased resistance in aqueous humor outflow. Elevated IOP causes the trabecular meshwork (HTM) to dilate through expansion of the spaces in the inner meshwork,[1] implicating the juxtacanalicular region (JCT) of the HTM at Schlemm's canal (SC) as the principal site of outflow resistance. Analysis of the JCT/SC reveals a region rich in extracellular matrix (ECM) components.[2,3] Excess synthesis of laminin, collagen IV, cross-linked fibronectin, tissue transglutaminase (a cross-linking enzyme), and protein adducts caused by lipid oxidation have been identified in glaucomatous meshworks, suggesting that these changes contribute to outflow resistance.[4] Studies have also correlated an increase in outflow resistance with elevated glycosaminoglycan (GAG) expression in HTM cells, which results in a shift in the ratio of chondroitin sulfate to hyaluronic acid.[5] We have identified multiple splice variants of chondroitin sulfate-substituted versican in HTM cells, which is thought to play a role in regulating IOP and have suggested that changes in the ratios of these spliced forms are related to reduced outflow. Thus, while the causes of glaucoma are not known or understood, changes in the HTM ECM and basement membrane are consistently reported with disease. Biophysical cues related to substrate topography have been shown to affect HTM cellular behavior.[6] Nanoscale to submicrometer topographic features influence HTM cell alignment, migration, and gene and protein expression. In addition to sensing substrate topography, cells sense and respond to the stiffness (typically expressed in terms of elastic modulus) of the underlying substrate.[7–9] Fibroblasts and osteoblasts change their stiffness by cytoskeletal reorganization to adapt to changes in substrate modulus.[10,11] Substrate modulus also affects cell alignment, migration, proliferation, and differentiation.[9,12–20] A change in substrate modulus is thought to have a role in disease development and has been implicated in vascular and muscle disease,[8,13,21–24] osteoarthritis,[25] liver fibrosis,[26,27] and tumor cell migration.[28]

Atomic force microscopy (AFM) has been useful in imaging and characterizing soft biological materials.[29] The force sensitivity and the spatial resolution available with AFM nanoindentation allow measurement of the local elastic modulus of soft biological materials and investigation of sample heterogeneities across small size scales. AFM has been successfully used for determining the mechanical properties of many tissues and cells.[29–41] We hypothesized that changes in the ECM observed in glaucoma results in an increase in local stiffness (increase in modulus) of the tissue and that this increase, in turn, decreases outflow facility from the eye. Using AFM, we found the modulus of the HTM to be substantially increased in glaucomatous globes, and modeling exercises sug-

From the [1]Department of Chemical and Biological Engineering, University of Wisconsin-Madison, Madison, Wisconsin; the Departments of [2]Biomedical Engineering and [3]Pathology, Microbiology, and Immunology, the [6]Department of Ophthalmology and Vision Science, School of Medicine, and the [7]Department of Surgical and Radiological Sciences, School of Veterinary Medicine, University of California, Davis, Davis, California; the [4]Casey Eye Institute, Oregon Health and Science University, Portland, Oregon; and the [5]Department of Ophthalmology, Mayo Clinic, Rochester, Minnesota.

Supported by the National Institutes of Health National Eye Institute Grants R01EY019475 (PR), 5R01EY016134 (CJM), EY07065 (MPF), EY15736 (MPF), EY003279 (TSA), EY008247 (TSA), and EY010572 (TSA); an Interagency Personnel Act grant (PR); and National Cancer Institute Grant 1R01CA133567–01 (CJM).

Submitted for publication August 4, 2010; revised October 27 and November 12, 2010; accepted November 14, 2010.

Disclosure: **J.A. Last**, None; **T. Pan**, None; **Y. Ding**, None; **C.M. Reilly**, None; **K. Keller**, None; **T.S. Acott**, None, **M.P. Fautsch**, None; **C.J. Murphy**, None; and **P. Russell**, None

*Each of the following is a corresponding author: Christopher J. Murphy, Department of Surgical and Radiological Sciences, School of Veterinary Medicine, 2112 Tupper Hall, University of California, Davis, Davis, CA 95616; cjmurphy@ucdavis.edu.

Paul Russell, Department of Surgical and Radiological Sciences, School of Veterinary Medicine, 2112 Tupper Hall, University of California, Davis, Davis, CA 95616; prussell@ucdavis.edu.

gest that this increase in modulus directly results in a decrease in aqueous outflow facility.

METHODS

Sample Preparation

Human donor eyes or corneal buttons determined unsuitable for transplantation were obtained from several eye banks. The donor eyes were managed in compliance with the tenets of the Declaration of Helsinki for research involving human tissue. In general, the glaucomatous samples were obtained without detailed information on the type of glaucoma, the extent of disease, or the medications used for treatment. Information with regard to the type of glaucoma was provided with only 3 of the 10 glaucoma samples, each with a diagnosis of primary open-angle glaucoma. The ages of the donors ranged from 32 to 92 years. The tissues were maintained in corneal storage medium (Optisol; Chiron Ophthalmics Irvine, CA) at 4°C before they were dissected to remove the HTM. The samples were prepared by dissection of the iris and uveal tissue with an ophthalmic knife (Alcon Surgical, Fort Worth, TX). The HTM was sectioned with a razor blade to provide samples less than 1 cm in length, and the sections were removed from the angle with forceps. The tissue was oriented so that the SC side of the JCT was probed and was affixed in the trabecular region with cyanoacrylate glue in the center of a stainless-steel AFM disc. AFM analysis was performed in 1× phosphate-buffered saline (PBS). The average time from donation to analysis was 17.5 ± 10.7 days for normal and 7.4 ± 4.2 days for glaucomatous samples (Table 1).

To characterize the region of tissue investigated with the AFM, we processed multiple normal corneal buttons for histopathology at various stages of preparation. Donor tissues were processed for routine histology as wedges of intact limbus, wedges of limbus after sharp dissection of uveal tissue, isolated HTM (longitudinal and cross section), and wedges of limbus after HTM isolation. All samples were fixed for 24 to 48 hours and processed routinely, and sections of isolated HTM were oriented for either longitudinal or cross-sectional sampling. After they were embedded, the samples were sectioned at 4 μm and stained with hematoxylin and eosin.

Instrumentation

Force curves were acquired with a scanning probe microscope (Nanoscope IIIa Multimode; Veeco Instruments, Inc., Santa Barbara, CA). The samples were transferred to the AFM without drying and placed in a commercially available liquid cell (Veeco Instruments, Inc.). Silicon nitride cantilevers with a borosilicate sphere as the tip (1 μm radius; Novascan Technologies, Inc., Ames, IA) were used to sample a large area of the HTM. The nominal spring constant of the cantilevers was 0.06 N/m. Force curves were obtained on at least 10 different locations, at either random locations on the sample or in a line with each measurement location separated by approximately 50 μm. Data exhibiting nonlinear behavior or a large adhesion with the surface were not included in the analysis, and a minimum of three locations were used to calculate the mean elastic modulus. In addition, when data were acquired at random locations, a minimum of three force curves were obtained at each location. Each force curve was taken at a rate of 2 μm/s.

Data Analysis

The force curves were analyzed with the Hertz model for a sphere in contact with a flat surface, by force curve analysis software (PUNIAS; Protein Unfolding and Nano-Indentation Analysis Software, http://punias.voila.net/). To obtain an accurate modulus, the optical sensitivity and the spring constant of each cantilever was determined. Optical sensitivity was measured as the slope of the force curve, taken in PBS, when the tip was in contact with a rigid surface. The optical sensitivity was used to convert cantilever deflection in volts to deflection in nanometers (x). Spring constants (k) were measured using Sader's method.[42] The force was determined by $F = kx$. The Hertz model provides a relationship between the loading force and the indentation, which for a spherical indenter is

$$F = \frac{4}{3}\frac{E}{1-\nu^2}\sqrt{R}\delta^{3/2} \quad (1)$$

where F is the loading force in Newtons, ν is Poisson's ratio (assumed to be 0.5), δ is the indentation depth, E is the elastic modulus in Pascals, and R is the radius of the tip. The values obtained from the force curve are z, z_0, d, and d_0, where z is the piezo displacement, d is the cantilever deflection, and z_0 and d_0 are the values at initial contact of the tip with the sample. These values can be used to calculate the indentation, which is given by

$$\delta = (z - z_0) - (d - d_0). \quad (2)$$

Using these equations and knowing that $F = k(d - d_0)$, where k is the cantilever spring constant, gives an equation for E

$$E = \frac{3}{4}\frac{k(d-d_0)(1-\nu^2)}{\sqrt{R}[(z-z_0)-(d-d_0)]^{3/2}}. \quad (3)$$

Models to Describe Flow

In the combined biomechanical and biofluidic model, the HTM is considered to be an elastic, porous membrane (36 mm in length, 0.3 mm in width, and 50 μm in thickness) with parallel cylindrical micropores embedded (with the original porous diameter of 1 μm and the porosity of 350/mm^2 chosen, to be within the range reported in the literature[43]). The IOP causes the HTM to

TABLE 1. Donor Age and Elastic Modulus for Normal and Glaucomatous Samples

Donor Age (y)	Days from Donation to Measurement	E ± SD Normal (kPa)	Range of E (kPa)	*n*	Donor Age (y)	Days from Donation to Measurement	E ± SD Glaucomatous (kPa)	Range of E (kPa)	*n*
32	NA	4.8 ± 2.4	1.3–7.6	5	72	6	102.6 ± 111.4	1.4–329.7	19
39	27	3.4 ± 4.7	0.6–16	10	76*	13	122.4 ± 111.5	36.4–382.8	8
56	30	1.9 ± 1.8	0.7–6.7	10	76*	13	138.4 ± 148.0	1.7–565.3	34
61	NA	1.7 ± 0.9	0.5–3.4	7	79	5	76.8 ± 124.4	0.8–552.0	22
69	17	2.1 ± 1.9	0.5–9.3	24	82	7	65.7 ± 33.5	23.2–126.6	14
70	30	3.2 ± 1.9	1.0–7.0	21	85	16	29.6 ± 52.0	0.5–206.9	24
77	13	4.0 ± 2.2	1.8–6.1	3	87	4	70.2 ± 121.3	2.0–243.0	25
78	15	6.5 ± 2.9	1.6–10.0	7	87*	11	78.5 ± 80.5	1.3–315.8	28
83	4	8.8 ± 2.4	4.4–8.8	13	92	4	73.2 ± 71.8	5.3–178.5	5
83	4	3.5 ± 1.3	1.6–5.4	13	92	4	50.4 ± 53.0	1.5–142.5	9

The time from donation to measurement indicates the length of time the samples were stored in cornea preservative. *n,* the number of measurements taken on each donor sample.

* Donors with primary open-angle glaucoma.

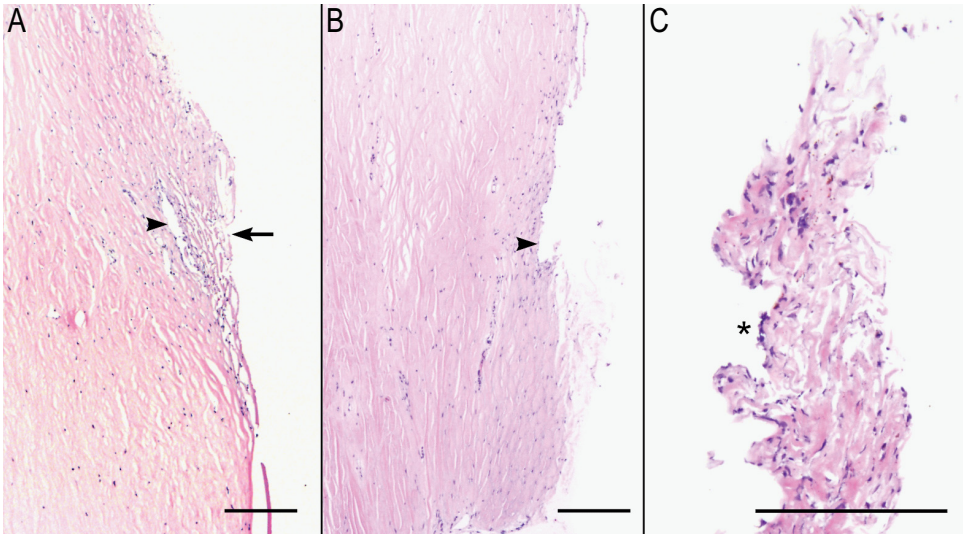

FIGURE 1. Histology of HTM throughout the isolation process. (**A**) Section of a donor cornea with HTM in situ. *Arrow*: the inner aspect of the HTM. *Arrowhead*: the outer wall of SC. (**B**) Donor cornea after removal of the HTM. *Arrowhead*: the outer wall of SC. (**C**) Isolated HTM after removal. The tissue is somewhat compressed (artifact). (✱) The inner wall of SC, the surface at which elastic modulus measurements were made. H&E; Magnification (**A**, **B**) ×4; (**C**) ×10; scale bar, 200 μm.

bow outward, which leads to the enlargement of the pore size. The size of micropore is a function of the elastic modulus of HTM (E) and aqueous outflow rate (Q), which can be derived from the following equations. Taking the HTM as a thin, elastic, porous membrane, the assumption of a thin plate with small deflections is applied, in which the normal stresses transverse to the plate (HTM) are disregarded.[44] Under the external pressure difference, the HTM (of length l, width w, and thickness t) deforms into a spherical shape with a central angle of 2α. The deflection of the HTM membrane can be related to the IOP (ΔP) acting on the HTM and the elastic modulus. According to Laplace's equation, the relationship among IOP, geometrical parameters, and material properties of the HTM can be expressed as

$$\Delta P = T\left(\frac{\sin\alpha}{l/2} + \frac{\sin\alpha}{w/2}\right) = 2T\sin\alpha\left(\frac{1}{l} + \frac{1}{w}\right) \approx \frac{2T\sin\alpha}{w} \quad (4)$$

where T represents internal tension parallel to the HTM and the length of the HTM is much greater than the width. Furthermore, the internal tension can be derived from the strain–stress relationship, which leads to the governing equation

$$\frac{E}{1-\gamma^2}\left(\frac{a}{\sin\alpha} - 1\right) = \frac{w\Delta P}{2t\sin\alpha} \quad (5)$$

where γ is Poisson's ratio. As can be seen, the central angle is a function of the IOP and the elastic modulus of the HTM. Eventually, the overall dynamic fluidic resistance of the HTM membrane can be calculated as

$$R = \frac{IOP}{Q} = \frac{8\mu t}{NA\pi r^4} = \frac{8\pi\mu t}{NAA_c(r,\alpha)^2} \quad (6)$$

where the aqueous outflow rate (Q) ranges from 2 to 3 μL/min and μ is the aqueous viscosity. Other structural parameters include the overall area and thickness of JCT (A and t), the porous density (N), as well as the area of an individual micropore (A_c), which can be calculated from the original pore size and the central angle of the HTM. Thus, the "effective" flow pathway leads to t/NA, or 0.013 μm, as modeled in this article.

RESULTS

Histologic examination of donor corneal buttons confirmed the presence of HTM and SC tissue in all the buttons examined (Fig. 1A). Tissues removed via sharp dissection were largely ciliary body muscle and pigmented uvea. Isolated HTM was difficult to orient precisely for histology, but all samples were confirmed to be composed predominantly of HTM beams and cells, with variable, but typically small, amounts of scleral collagen, rare melanocytes and, in one case, remnants of Descemet's membrane. The inner wall of SC was multifocally/segmentally absent from the postisolation corneal buttons (Fig. 1B). HTM tissue was identified in well-oriented regions of isolated HTM tissue, and the inner wall of SC was identified in some sections (Fig. 1C).

AFM force curves, a plot of cantilever deflection versus z piezo movement, were obtained on HTM from normal and glaucomatous donors. The force curves obtained on these tissues, taken from the internal surface of SC, had the same characteristics as those obtained on other soft, elastic materials.[45,46] In general, the force curves consisted of a straight-line

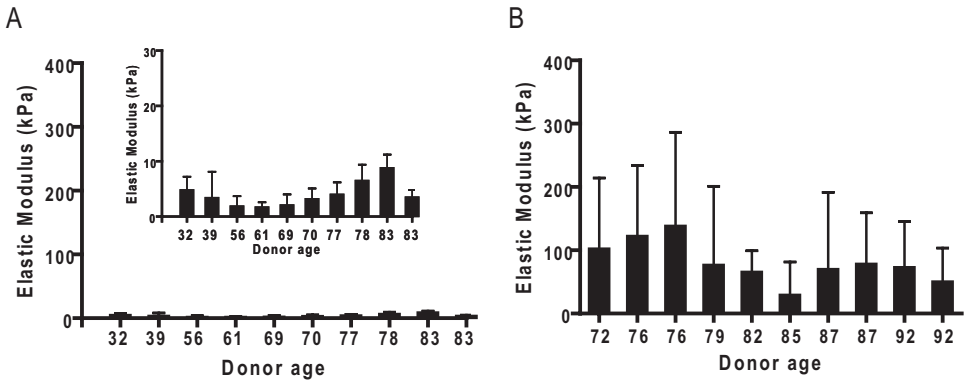

FIGURE 2. HTM elastic modulus versus donor age. AFM nanoindentation was used to determine the mean elastic modulus for (**A**) normal (*inset*: data plotted on a smaller y scale) and (**B**) glaucomatous HTM samples.

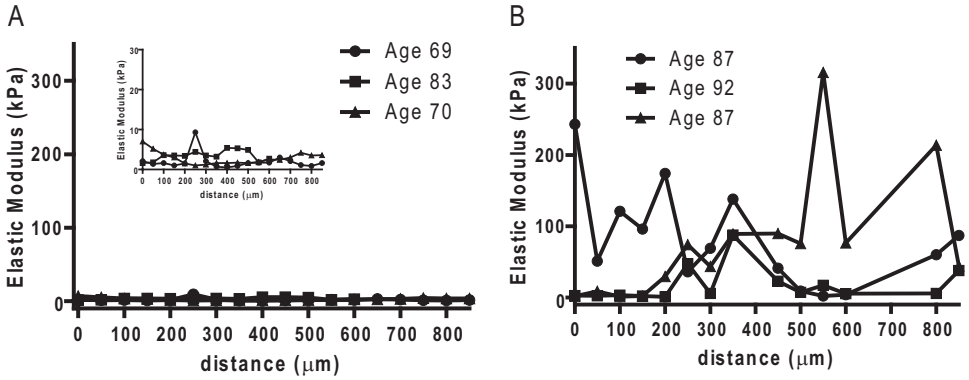

FIGURE 3. Force curve measurements taken every 50 μm on (**A**) normal (*inset*: data plotted on smaller y scale) and (**B**) glaucomatous HTM. Elastic modulus of the HTM every 50 μm along the tissue show little variation in normal HTM but a wide variation in glaucomatous HTM.

approach when the tip was still away from the surface. As the tip came into contact with the surface, there was a gradual increase in the deflection of the cantilever, as expected for soft samples. Large pull-off forces were not typically observed as the tip was retracted from the surface, indicating negligible adhesion of the tip with the HTM. The approach and retract curves overlapped, indicating an absence of viscoelastic effects at the indentation rate used (1 Hz).

Measurement of the elastic modulus in normal HTM (n = 10; mean age, 65 years; range, 32–83 years) ranged from 1.7 to 8.8 kPa (mean, 4.0 ± 2.2 kPa; Table 1, Fig. 2). In comparison, glaucomatous HTM (n = 10; mean age, 84 years; range, 72–92 years) had a significant increase in elastic modulus ranging from 29.6 to 138.4 kPa (mean, 80.8 ± 32.5 kPa; $P < 0.0001$; Fig. 2). Analysis of 50-μm intervals along the glaucomatous HTM revealed large variations ranging from less than 10 kPa to greater than 200 kPa. In contrast, minimal variations in elastic modulus were identified in normal HTM, with all values less than 15 kPa (Fig. 3).

We used a mathematical model to determine whether the change in modulus between normal and glaucomatous HTM might influence the facility of aqueous outflow. A mathematical model has been established to evaluate the impact of modulating intrinsic stiffness on outflow resistance. In this model, we consider the HTM as an elastic porous membrane with conjugated biomechanical and biofluidic responses. Figure 4 shows that the increase in HTM stiffness increased the flow resistance of the JCT. This increase was due to a pressure elevation across the JCT/SC layer that enlarged the pore size, which was inversely proportional to the fourth power of the outflow resistance. As a consequence, the pathologically increased stiffness of the HTM in glaucomatous eyes led to considerably higher outflow resistance than that in the normal control group. Our model showed a similar trend of the outflow facility's dependence on IOP/flow rate variation, as predicted by previous biomechanical models.[47] While this model is one of several that could be applied, in all conventional models, a change in facility would be substantially influenced by the changes in elastic modulus measured between the normal and diseased HTM.

DISCUSSION

This study reveals for the first time a significant increase in HTM stiffness related to glaucoma. It is important to note that stiffness in this case refers to an intrinsic material property that is independent of the extrinsic forces generated by alterations in fluid dynamics. This finding is consistent with the reported changes that have been observed in the glaucomatous HTM, by either microscopy or gene and protein expression changes. In other work, we have demonstrated that a change in substratum stiffness profoundly alters the modulus of the overlying HTM cells (data not shown). Our data support a model for disease onset and progression in glaucoma wherein dysregulation of the ECM observed with glaucoma is associated with alterations in the stiffness of the HTM and associated cells which, in turn, cause an increase in resistance to aqueous humor outflow (Fig. 5). These interactions set up a vicious cycle that, without therapeutic intervention, would result in a progressive increase in IOP and associated visual field loss. We note that in this scenario there are two distinct contributing factors to the stiffness of the HTM, an intrinsic stiffness of the ECM (i.e., an intrinsic attribute at rest, determined by the constituents of the ECM as well as their three-dimensional nanoscale organization, and a dynamic component [stretch] induced by increasing the pressure gradient across the HTM with decreasing outflow).

The variation of the modulus when taken in 50-μm intervals along the glaucomatous HTM was unexpected. The presence of an elastic modulus less than 10 kPa indicates that the disease process does not uniformly affect the HTM and suggests that relatively unaffected regions persist within the glaucomatous HTM. This finding is consistent with the concept of segmental flow of aqueous humor out of the eye.[48,49] The concept of segmental flow suggests that there is a nonuniform outflow through the meshwork into SC that results in a spatial variation in outflow facility around the circumference of the drainage pathway. Our results suggest that segmental flow is profoundly

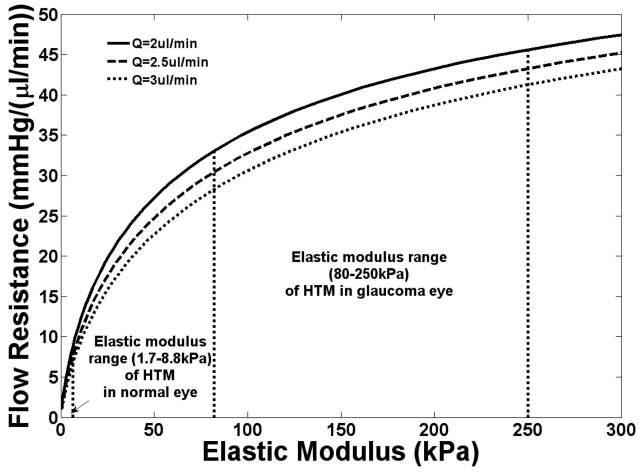

FIGURE 4. Results from a mathematical modeling of a membrane with 1-μm pores showing the change in flow resistance with increasing elastic modulus. The curves were plotted for three different flows of liquid through the pores. These flow rates are similar to those reported for aqueous humor outflow. The model demonstrates that there is an increase in flow resistance with increasing elastic modulus.

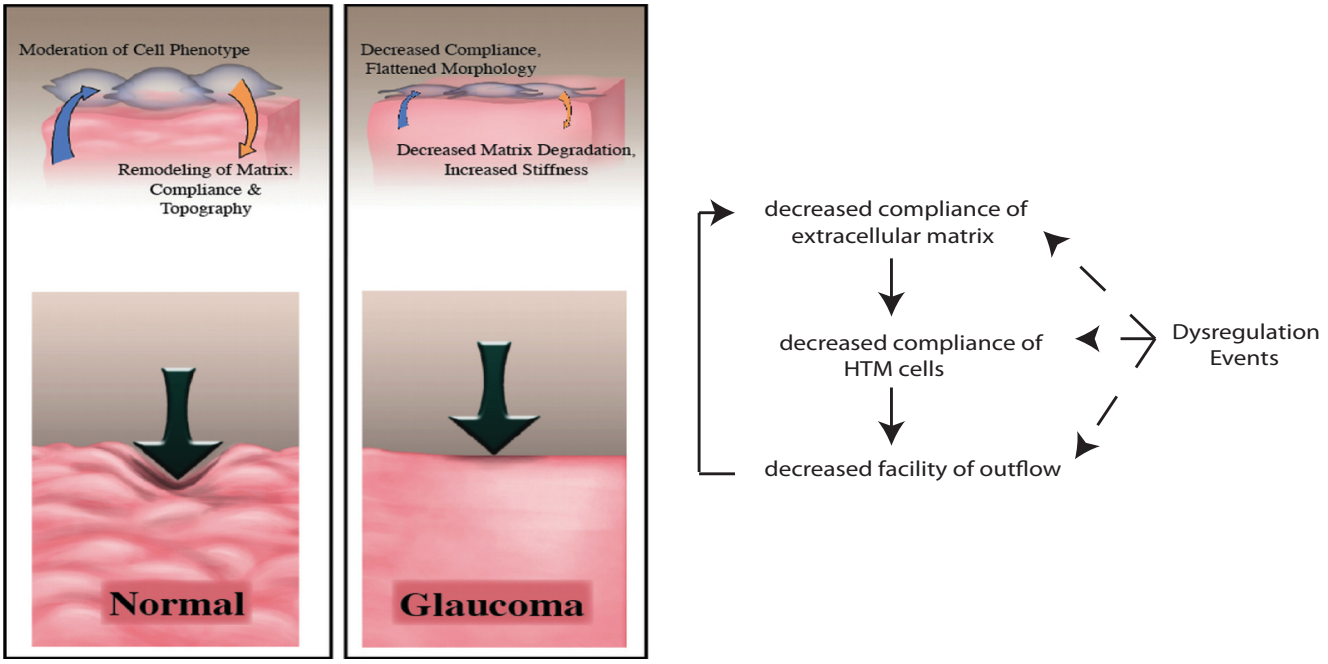

FIGURE 5. Interplay between the biophysical properties of the ECM, HTM cells, and outflow facility. Normal ECM of the meshwork is compliant and contains topographic features with which the HTM cells can interact. In glaucoma, the matrix is stiff causing increased stiffness of the HTM cells and reduced matrix degradation. The central concept of this proposal is that with initiation or progression of glaucoma, dysregulation events can initiate a feedback loop that increases stiffness of the matrix thereby increasing stiffness of the HTM cells and lowering outflow facility.

altered by glaucoma. While information on the severity of the disease for each donor is unknown, we believe that fewer and/or smaller regions having a normal (lower) modulus would be observed with disease progression.

While there are multiple mathematical models that have been and can be used to establish a correlation of modulus and outflow facility, the changes observed in local stiffness of the HTM with disease are in concert with a decreased facility of outflow. There are obvious limitations in our mathematical model as there are with all models. First, the thin plate assumption oversimplifies the real situation in the eye, in which normal stresses may play a significant role. Also, the deformation of the HTM may not be perfectly spherical. We consider the HTM to be purely elastic, and we do not include any viscosity parameters that would more accurately represent real biomaterials. The interesting aspect of the model is that basic physical phenomena are used to predict outflow facility in the HTM. Our model consists of Laplace's law, an elastic strain–stress relationship, and the thin membrane model with a small deflection. We do not consider any biological effects in the model.

These findings strongly suggest that the change in elastic modulus of the HTM is a factor that contributes to the increased IOP that is often observed in POAG. These results point to the development of novel approaches for therapeutic intervention designed to lower the elastic modulus in glaucomatous HTM. Indeed, recent results from our laboratory reveal that changes in substrate elastic modulus dramatically affect cellular responses to therapeutic agents.[50]

It should be noted that while the age ranges of the normal and glaucomatous samples are different, there is substantial overlap in these sets of data between the ages of 72 and 83. Normal samples with donor ages from 70 to 83 continue to have a mean elastic modulus less than 10 kPa. In addition, the normal samples show no statistically significant correlation of elastic modulus with age ($P = 0.3614$). Each glaucomatous sample with a donor age from 72 to 82, however, had a mean elastic modulus greater than 60 kPa. These observations suggest that it is the presence of glaucoma and not simply an aging of the tissue that is responsible for the increase in the elastic modulus. In addition to the variation in ages, it should be noted that, within each set of samples, the number of days from date of death to analysis also varied. Measurements were completed on normal samples within 30 days of the date of death, ranging from 4 to 30 days and on the glaucomatous samples within 16 days of the date of death, ranging from 4 to 16 days. A correlation analysis of the elastic modulus and the number of days from the date of death revealed no statistically significant correlation for either the normal ($P = 0.12$) or glaucomatous ($P = 0.95$) samples.

Acknowledgments

The authors thank Nicholas Abbott for use of the AFM.

References

1. Johnstone M, Grant W. Pressure-dependent changes in structure of the aqueous outflow system of human and monkey eyes. *Am J Ophthalmol.* 2008;75:365–383.
2. Acott TS, Kelley MJ. Extracellular matrix in the trabecular meshwork. *Exp Eye Res.* 2008;86:543–561.
3. Fuchshofer R, Welge-Lussen U, Lutjen-Drecoll E. The effect of TGF-beta2 on human trabecular meshwork extracellular proteolytic system. *Exp Eye Res.* 2003;77:757–765.
4. Tovar-Vidales T, Roque R, Clark AF, Wordinger RJ. Tissue transglutaminase expression and activity in normal and glaucomatous human trabecular meshwork cells and tissues. *Invest Ophthalmol Vis Sci.* 2008;49:622–628.
5. Knepper PA, Goossens W, Hvizd M, Palmberg PF. Glycosaminoglycans of the human trabecular meshwork in primary open-angle glaucoma. *Invest Ophthalmol Vis Sci.* 1996;37:1360–1367.
6. Russell P, Gasiorowski JZ, Nealy PF, Murphy CJ. Response of human trabecular meshwork cells to topographic cues on the nanoscale level. *Invest Ophthalmol Vis Sci.* 2008;49:629–635.

7. Discher DE, Janmey P, Wang YL. Tissue cells feel and respond to the stiffness of their substrate. *Science.* 2005;310:1139–1143.
8. Engler A, Bacakova L, Newman C, Hategan A, Griffin M, Discher D. Substrate compliance versus ligand density in cell on gel responses. *Biophys J.* 2004;86:617–628.
9. Georges PC, Janmey PA. Cell type-specific response to growth on soft materials. *J Appl Physiol.* 2005;98:1547–1553.
10. Solon J, Levental I, Sengupta K, Georges PC, Janmey PA. Fibroblast adaptation and stiffness matching to soft elastic substrates. *Biophys J.* 2007;93:4453–4461.
11. Takai E, Costa KD, Shaheen A, Hung CT, Guo XE. Osteoblast elastic modulus measured by atomic force microscopy is substrate dependent. *Ann Biomed Eng.* 2005;33:963–971.
12. Bergethon PR, Trinkaus-Randall V, Franzblau C. Modified hydroxyethylmethacrylate hydrogels as a modelling tool for the study of cell-substratum interactions. *J Cell Sci.* 1989;92:111–121.
13. Engler AJ, Griffin MA, Sen S, Bonnemann CG, Sweeney HL, Discher DE. Myotubes differentiate optimally on substrates with tissue-like stiffness: pathological implications for soft or stiff microenvironments. *J Cell Biol.* 2004;166:877–887.
14. Gunn JW, Turner SD, Mann BK. Adhesive and mechanical properties of hydrogels influence neurite extension. *J Biomed Mater Res A.* 2005;72:91–97.
15. Koh WG, Revzin A, Simonian A, Reeves T, Pishko M. Control of mammalian cell and bacteria adhesion on substrates micropatterned with poly(ethylene glycol) hydrogels. *Biomed Microdevices.* 2003;5:11–19.
16. Semler EJ, Lancin PA, Dasgupta A, Moghe PV. Engineering hepatocellular morphogenesis and function via ligand-presenting hydrogels with graded mechanical compliance. *Biotechnol Bioeng.* 2005;89:296–307.
17. Shin H, Zygourakis K, Farach-Carson MC, Yaszemski MJ, Mikos AG. Modulation of differentiation and mineralization of marrow stromal cells cultured on biomimetic hydrogels modified with Arg-Gly-Asp containing peptides. *J Biomed Mater Res A.* 2004;69:535–543.
18. Wallace C, Jacob JT, Stoltz A, Bi J, Bundy K. Corneal epithelial adhesion strength to tethered-protein/peptide modified hydrogel surfaces. *J Biomed Mater Res A.* 2005;72:19–24.
19. Wozniak MA, Desai R, Solski PA, Der CJ, Keely PJ. ROCK-generated contractility regulates breast epithelial cell differentiation in response to the physical properties of a three-dimensional collagen matrix. *J Cell Biol.* 2003;163:583–595.
20. Xia W, Liu W, Cui L, et al. Tissue engineering of cartilage with the use of chitosan-gelatin complex scaffolds. *J Biomed Mater Res B Appl Biomater.* 2004;71:373–380.
21. Campbell GR, Chamley-Campbell JH. Smooth-muscle phenotypic modulation: role in atherogenesis. *Med Hypotheses.* 1981;7:729–735.
22. Glukhova MA, Koteliansky VE. Integrins, cytoskeletal and extracellular matrix proteins in developing smooth muscle cells of human aorta. In: Schwartz SM, Mecham RP, ed. *The Vascular Smooth Muscle Cell Molecular and Biological Responses to the Extracellular Matrix.* New York: Academic Press; 1995:37–79.
23. Stedman HH, Sweeney HL, Shrager JB, et al. The Mdx mouse diaphragm reproduces the degenerative changes of Duchenne muscular-dystrophy. *Nature.* 1991;352:536–539.
24. Stenmark KR, Mecham RP. Cellular and molecular mechanisms of pulmonary vascular remodeling. *Annu Rev Physiol.* 1997;59:89–144.
25. Genes NG, Rowley JA, Mooney DJ, Bonassar LJ. Effect of substrate mechanics on chondrocyte adhesion to modified alginate surfaces. *Arch Biochem Biophys.* 2004;422:161–167.
26. Georges PC, Hui JJ, Gombos Z, et al. Increased stiffness of the rat liver precedes matrix deposition: implications for fibrosis. *Am J Physiol Gastrointest Liver Physiol.* 2007;293:G1147–G1154.
27. Wells RG. The role of matrix stiffness in hepatic stellate cell activation and liver fibrosis. *J Clin Gastroenterol.* 2005;39:S158–S161.
28. Zaman MH, Trapani LM, Siemeski A, et al. Migration of tumor cells in 3D matrices is governed by matrix stiffness along with cell-matrix adhesion and proteolysis. *Proc Natl Acad Sci USA.* 2006;103:10889–10894.
29. Last JA, Russell P, Nealey PF, Murphy CJ. The applications of atomic force microscopy to vision science. *Invest Ophthalmol Vis Sci.* 2010;51:6083–6094.
30. Bowen WR, Lovitt RW, Wright CJ. Application of atomic force microscopy to the study of micromechanical properties of biological materials. *Biotechnol Lett.* 2000;22:893–903.
31. Canetta E, Adya AK. Atomic force microscopy: applications to nanobiotechnology. *J Indian Chem Soc.* 2005;82:1147–1172.
32. Docheva D, Padula D, Popov C, Mutschler W, Clausen-Schaumann H, Schieker M. Researching into the cellular shape, volume and elasticity of mesenchymal stem cells, osteoblasts and osteosarcoma cells by atomic force microscopy. *J Cell Mol Med.* 2008;12:537–552.
33. Hsieh CH, Lin YH, Lin S, Tsai-Wu JJ, Herbert Wu CH, Jiang CC. Surface ultrastructure and mechanical property of human chondrocyte revealed by atomic force microscopy. *Osteoarthritis Cartilage.* 2008;16:480–488.
34. Ikai A. Nanobiomechanics of proteins and biomembrane. *Philos Trans R Soc Lond B Biol Sci.* 2008;363:2163–2171.
35. Jandt KD. Atomic force microscopy of biomaterials surfaces and interfaces. *Surf Sci.* 2001;491:303–332.
36. Li QS, Lee GY, Ong CN, Lim CT. AFM indentation study of breast cancer cells. *Biochem Biophys Res Commun.* 2008;374:609–613.
37. Mathur AB, Collinsworth AM, Reichert WM, Kraus WE, Truskey GA. Endothelial, cardiac muscle and skeletal muscle exhibit different viscous and elastic properties as determined by atomic force microscopy. *J Biomech.* 2001;34:1545–1553.
38. Rabinovich Y, Esayanur M, Daosukho S, Byer K, El-Shall H, Khan S. Atomic force microscopy measurement of the elastic properties of the kidney epithelial cells. *J Colloid Interface Sci.* 2005;285:125–135.
39. Rico F, Roca-Cusachs P, Gavara N, Farre R, Rotger M, Navajas D. Probing mechanical properties of living cells by atomic force microscopy with blunted pyramidal cantilever tips. *Phys Rev E Stat Nonlin Soft Matter Phys.* 2005;72:021914.
40. Sirghi L, Ponti J, Broggi F, Rossi F. Probing elasticity and adhesion of live cells by atomic force microscopy indentation. *Eur Biophys J.* 2008;37:935–945.
41. Wagh AA, Roan E, Chapman KE, et al. Localized elasticity measured in epithelial cells migrating at a wound edge using atomic force microscopy. *Am J Physiol Lung Cell Mol Physiol.* 2008;295:L54–L60.
42. Sader JE. Parallel Beam Approximation for V-shaped atomic-force microscope cantilevers. *Rev Sci Instrum.* 1995;66:4583–4587.
43. Ethier CR, Coloma FM, Sit AJ, Johnson M. Two pore types in the inner-wall endothelium of Schlemm's canal. *Invest Ophthalmol Vis Sci.* 1998;39:2041–2048.
44. Timoshenko S, Woinowsky-Krieger S. *Theory of Plates and Shells.* 2nd ed. New York: McGraw-Hill; 1987.
45. Cappella B, Dietler G. Force-distance curves by atomic force microscopy. *Surf Sci Rep.* 1999;34:1–104.
46. Clifford CA, Seah MP. Quantification issues in the identification of nanoscale regions of homopolymers using modulus measurement via AFM nanoindentation. *Appl Surf Sci.* 2005;252:1915–1933.
47. Ethier CR. The inner wall of Schlemm's canal. *Exp Eye Res.* 2002;74:161–172.
48. Buller C, Johnson D. Segmental variability of the trabecular meshwork in normal and glaucomatous eyes. *Invest Ophthalmol Vis Sci.* 1994;35:3841–3851.
49. Hann C, Bahler C, Johnson D. Cationic ferritin and segmental flow through the trabecular meshwork. *Invest Ophthalmol Vis Sci.* 2005;46:1–7.
50. McKee CT, Wood JA, Shah NM, et al. The effect of biophysical attributes of the ocular trabecular meshwork associated with glaucoma on the cellular response to therapeutic agents. *Biomaterials.* 2011;32:2417–2423.